Electronic supplementary information for

Self-templating growth of Sb_2Se_3@C microtube: A convention-alloying-type anode material for enhanced K-ion batteries

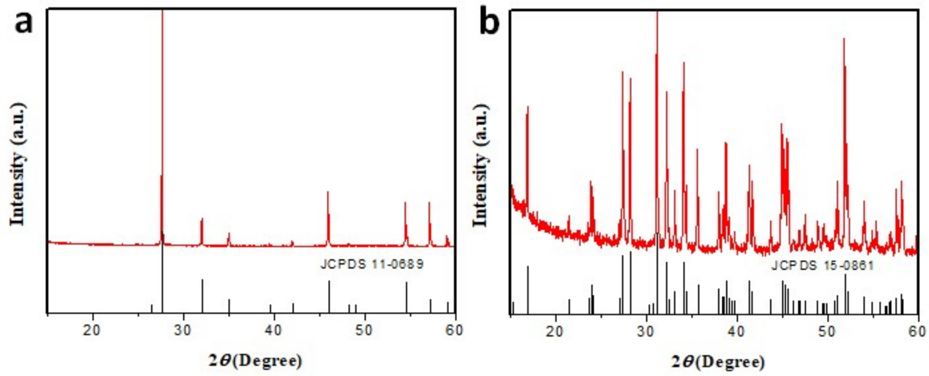

Fig.S1. (a-b) The XRD patterns of the selenide products obtained by using the Sb_2O_3 precursor and the commercial Sb powders as the Sb sources. As can be seen from the Fig.S1, when used the pure Sb_2O_3 precursor as Sb sources, no Sb_2Se_3 products is harvested (Fig.S1a), while when used the Sb_2O_3@RF as Sb sources, the Sb_2Se_3 products can be obtained (Fig.2a). In addition, when used the pure commercial Sb powders as Sb sources, Sb_2Se_3 products is also harvested (Fig.S1b). Therefore, it can be seen that the Sb_2O_3 is hardly transformed to Sb_2Se_3 without a reduction agent. For the Sb_2O_3@RF as Sb sources, the RF is firstly transformed to be carbon, and then acted a reducing agent to reduce the Sb_2O_3 to Sb. The new formation of Sb with high activity can react with the Se to produce the Sb_2Se_3 products.

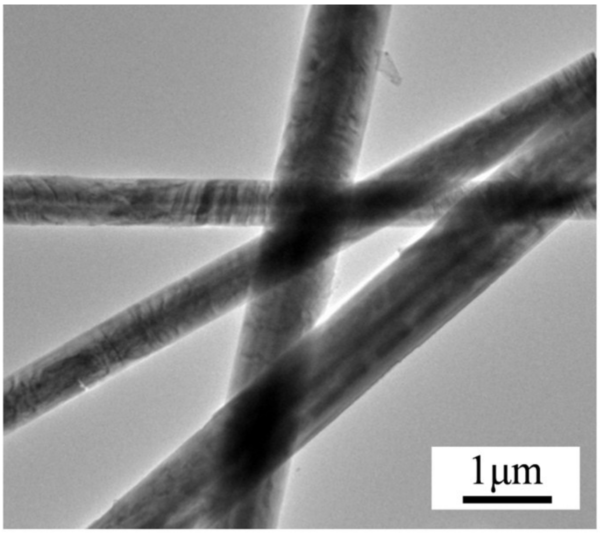

Fig.S2. The TEM image of the Sb_2O_3 precursor.

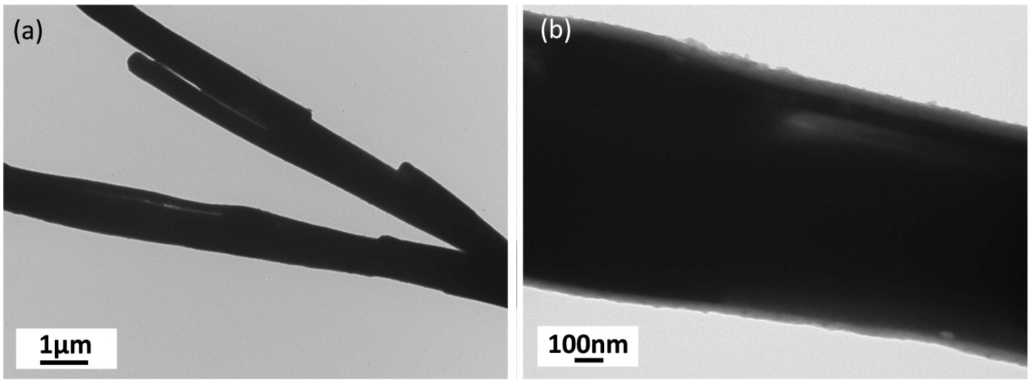

Fig. S3. (a-b) TEM images of the solid Sb_2Se_3@C submicrorods.

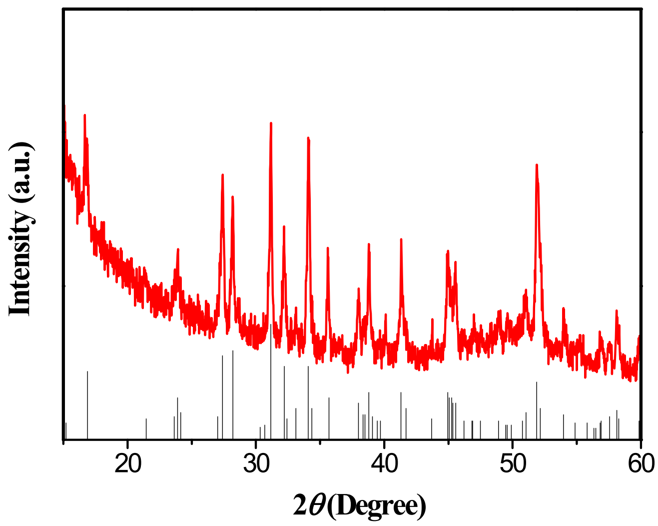

Fig. S4. XRD pattern of the solid Sb_2Se_3@C submicrorods.

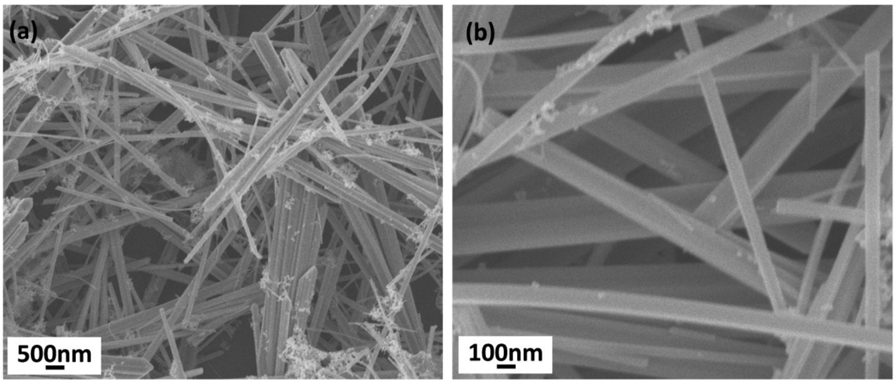

Fig. S5. (a-b) SEM images of solid Sb_2Se_3 submicrorods obtained by a hydrothermal method..

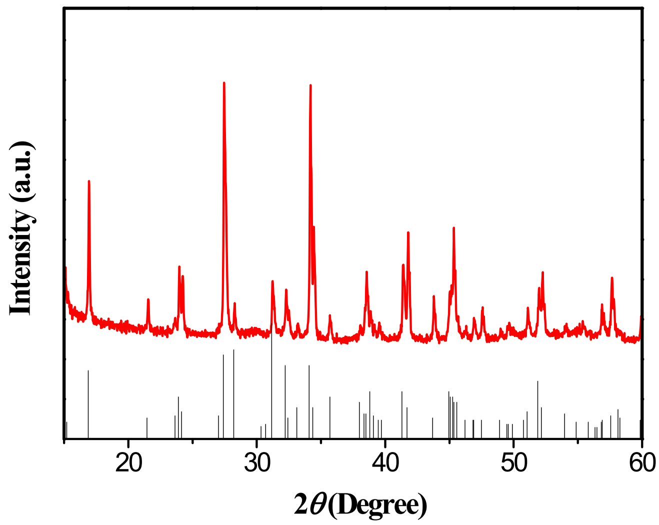

Fig. S6. XRD pattern of the solid Sb_2Se_3 submicrorods obtained by a hydrothermal method.

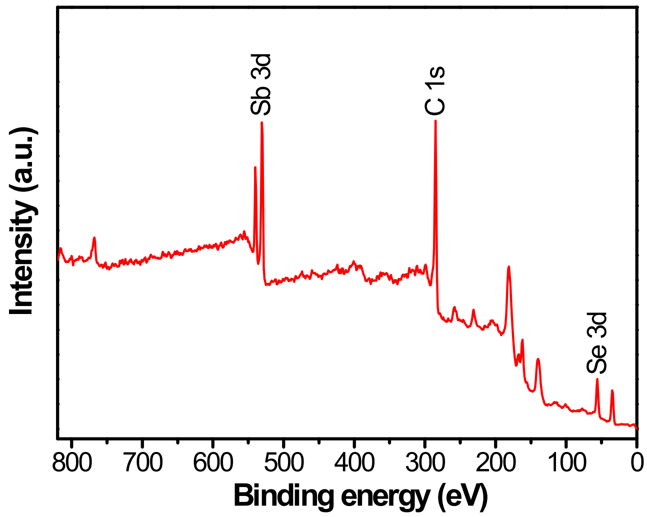

Fig. S7. The XPS of the hollow Sb_2Se_3@C submicrotubes.

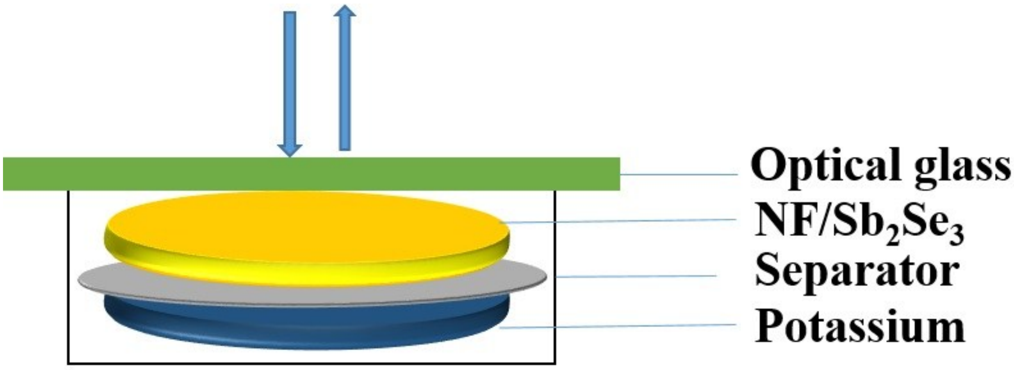

Fig. S8. Schematic of Raman cell setup (NF=Ni foil).

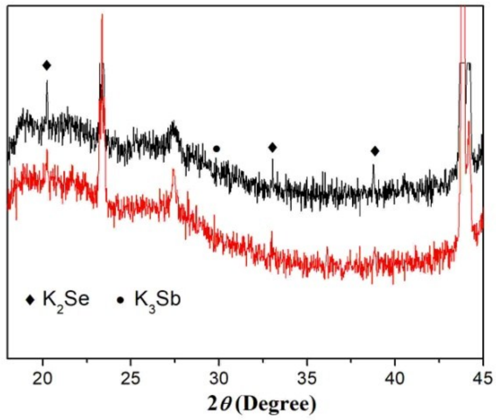

Fig. S9. The XRD pattern of the hollow Sb_2Se_3@C microtube electrode discharged at 0.05 V *vs* K^+/K.

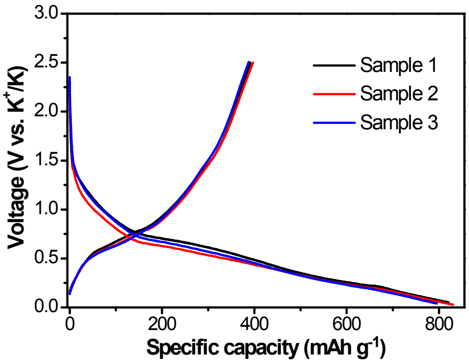

Fig.S10 The first charge/discharge curves of the hollow Sb_2Se_3@C microtube at 100 mA g^{-1}. These curves are obtained from three cells at similar testing condition.

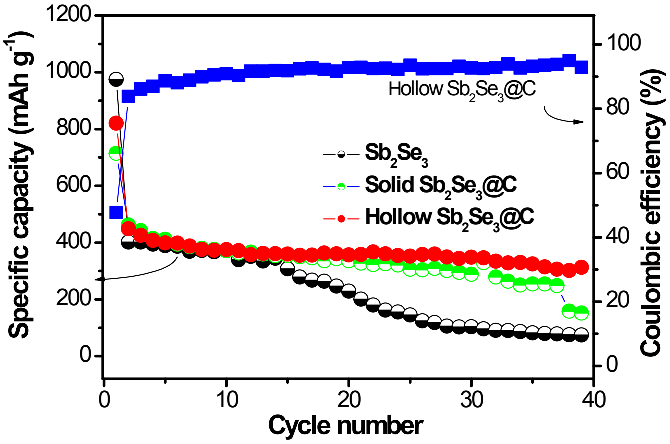

Fig. S11. Comparison of the galvanostatic cycling performance at a current density of 100 mA g^{-1}.

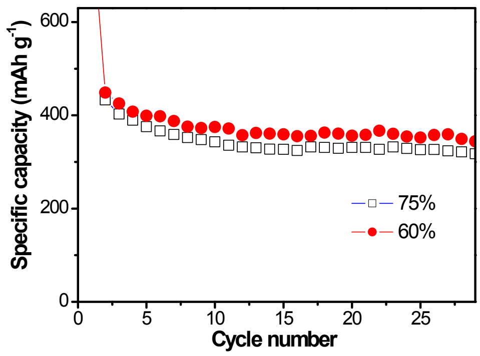

Fig.S12 Cycling performance of the hollow Sb_2Se_3@C microtube at 100 mA g^{-1} with active material content of 75 % (with 15% of conductive agent and 10% of binder). The red symbol imply the sample with 60% of active materials in agreement with Fig.4b.

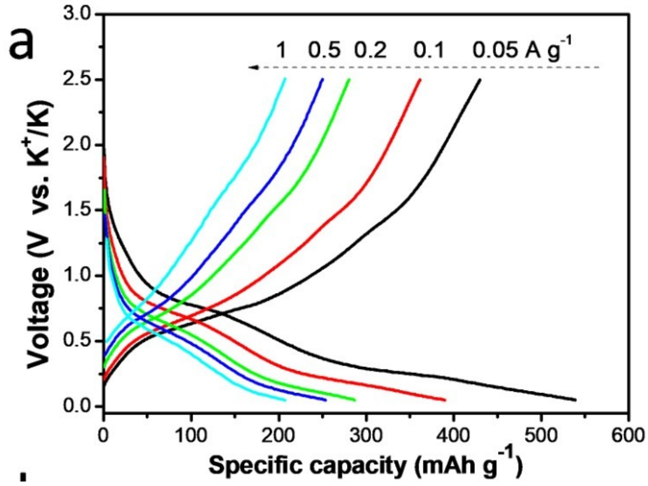

Fig. S13. (a) Rate charge/discharge curves of the hollow Sb_2Se_3@C microtubes at different current densities. (b) Comparison of the potassium storage performances of the hollow Sb_2Se_3@C microtubes and the previously reported selenide/sulfide-based anode materials in PIBs.

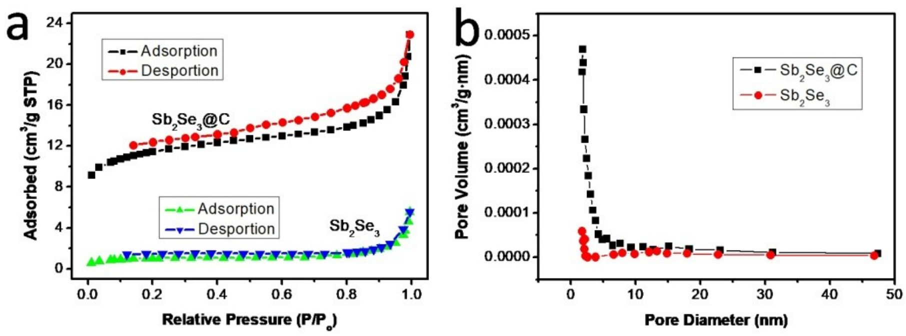

Fig.S14. (a) N_2 adsorbed curves and (b) pore volume of the hollow Sb_2Se_3@C microtubes and pure Sb_2Se_3 microrod electrode.

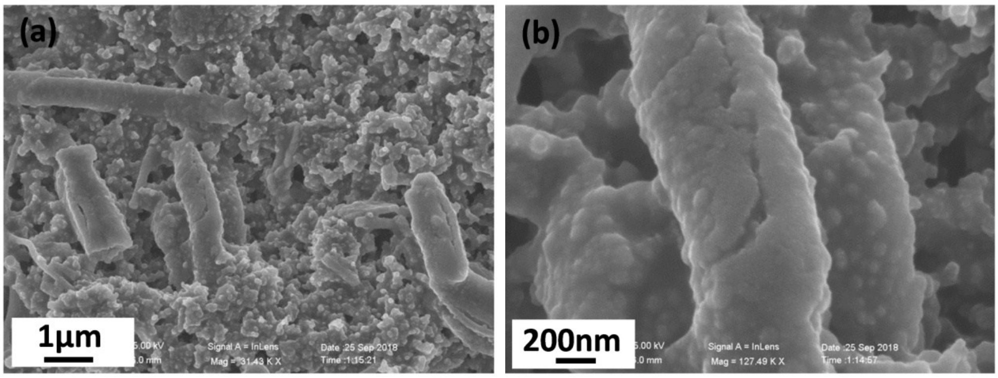

Fig.S15. SEM images of (a-b) the solid Sb_2Se_3@C submicrorod electrode.

References: